

PETROGRAPHIC CHARACTERIZATION AND PRELIMINARY MICROTHERMOMETRY OF THE HYDROTHERMAL SYSTEM AT FLYNN CREEK CRATER, TENNESSEE.

A. L. Gullikson¹, T. A. Gaither¹, K. A. Villarreal¹, and J. J. Hagerty¹, ¹USGS, Astrogeology Science Center, 2255 N Gemini Drive, Flagstaff, AZ, 86001.

Introduction: Flynn Creek crater is a ~3.8 km diameter, >200 m deep, flat-floored impact structure, with a central uplift and terraced crater rim [1]. It is believed that the impactor struck into a shallow sea (what is now north-central Tennessee), comprised of Ordovician-aged carbonates (i.e., limestone and dolomite) overlain on top of crystalline basement [1-4].

Based on the location and composition of the target rocks (i.e., marine carbonates) and energy produced from the impact, there is potential for an impact-induced hydrothermal system at Flynn Creek crater. This idea is of considerable scientific interest because of the implications for the origin and evolution of life on early Earth [5-6], and possibly on Mars [7-9]. Because of a drilling campaign carried out by USGS scientist Dr. David Roddy, which produced more than 3.8 km of nearly continuous core from 18 separate bore holes from Flynn Creek [10], we have the ability to address this scientific interest.

Hydrothermal activity at Flynn Creek: Evidence for hydrothermal alteration at Flynn Creek crater has been suggested by [3] and [11], but no definitive, quantitative studies have been published. Our work has been aimed at characterizing the hydrothermal mineral assemblage and the extent of hydrothermal activity at the Flynn Creek impact structure. Results from this work can be used as constraints for numerical modeling of the Flynn Creek impact event and contribute to the understanding of shallow marine-target impact structures.

With these goals in mind, areas with possible hydrothermal deposits were identified and selected based on our recent digital archival work for the Flynn Creek crater online database (<https://astrogeology.usgs.gov/facilities/flynn-creek-crater-sample-collection>). A total of 44 thin sections were made from drill cores located in the central uplift and moat for a detailed petrographic study of the Flynn Creek hydrothermal system. Subsequent preliminary microthermometry was then carried out at the USGS Denver Inclusion Analysis Laboratory to quantify the composition of the hydrothermal

fluids and its temperature. Located in the central uplift, 24 thin sections were prepared from drill core 12, ranging in depth from 287 m to 790 m, and 4 thin sections from drill core 13, ranging in depth from 450 m to 564 m. Located in the moat of the crater, 17 thin sections were prepared from drill core 7, ranging in depth from 340 m to 616 m.

Results: *Drill core 12.* A complete petrographic study was carried out on all thin sections from drill core 12. Samples contain various monomict and polymict lithic breccias. Only minor amounts of hydrothermal alteration were observed in the form of thin quartz and calcite veins.

Drill core 7. Currently 10 of the 17 thin sections from this core have been thoroughly characterized using a petrographic microscope and scanning electron microscope. Of the 10 thin sections, we have identified 3 samples that have evidence for hydrothermal activity. Two slides were sampled at similar depths, 504 – 507 m, and were observed to have a hydrothermal mineral assemblage of fluorite, barite, and calcite. The majority of fluorite crystals were fractured, ranging in size from ~50 to 100 μm and were only found in massive, anhedral calcite veins that cut through the fine-grained breccia matrix. Barite grains are euhedral to subhedral, prismatic crystals that display two types of texture; 1) crystals within the massive, anhedral calcite veins exhibit a radial, fan-shaped crystal habit, and 2) crystals found in fine-grained carbonate matrix, near calcite veins were dense clusters of individual prismatic crystals that sometimes formed penetration twins.

At a depth of ~563-567 m, euhedral to subhedral potassium feldspar (adularia), ~50 μm in size are found in a fine-grained carbonate matrix (containing both calcite and dolomite). All samples from the moat are dominantly polymict breccia with varying amounts of limestone, dolomite, and siltstone, and only a minor amount of hydrothermal minerals.

Drill core 13. Currently only 1 of the 4 thin sections has been fully characterized. This section was sampled at a depth of 559-562 m and has euhedral to subhedral fluorite crystals located

within a massive, anhedral calcite vein. Fluorite tend to cluster on the interior boundary of the calcite vein, near fragments of lithic dolomite.

Preliminary microthermometry: Two-phase (liquid + vapor) and single-phase (liquid) fluid inclusions were identified in fluorite, barite, and calcite, located in drill cores 13 and 7 (central uplift and moat, respectively). A total of 7 fluid inclusion assemblages were analyzed in fluorite (e.g., **Figure 1**) and 4 fluid inclusion assemblages in calcite. Fluid inclusions observed in barite were unfortunately too small to obtain any accurate measurements (i.e., <10 μm). Homogenization temperatures for both fluorite and calcite were measured to identify a minimum temperature of entrapment (T_e). To constrain the composition of the fluid and its salinity, melting temperatures (T_m) were measured for fluorite. Based on these measurements, there appears to be a lower T_e for one group of minerals (including both calcite and fluorite) ranging from 59-74 $^{\circ}\text{C}$, and a higher temperature group ranging from 97-124 $^{\circ}\text{C}$. Calcite sampled from the moat had a fairly narrow minimum range of T_e (62-70 $^{\circ}\text{C}$), however, calcite sampled from the central uplift represented both lower temperatures (67 $^{\circ}\text{C}$) and higher temperatures (100-106 $^{\circ}\text{C}$) of entrapment. Apart from one fluid inclusion assemblage measured in fluorite, fluorite typically represents a higher T_e compared to calcite (i.e., 97-125 $^{\circ}\text{C}$). T_m measurements ranged from -5 $^{\circ}\text{C}$ to -20 $^{\circ}\text{C}$ in fluorite. In addition to T_m , a eutectic temperature of -65 $^{\circ}\text{C}$ was measured for one fluorite inclusion assemblage, which suggests that calcite and fluorite precipitated in a saline-rich fluid, with the addition of Ca and/or Mg in the fluid.

Conclusions and Future Work: Thin sections from drill cores located in both the central uplift and moat of Flynn Creek crater show evidence of hydrothermal alteration in the form of fluorite, barite, calcite, and adularia. Preliminary microthermometry results are consistent with models proposed by [7] and [12], which describes the central uplift of the crater having a higher residual temperature compared to the moat. Data suggest that fluorite precipitated first at higher temperatures, followed by calcite. The salinity and composition of the fluid inclusions also suggest the origin of the fluid is seawater with an enrichment of Ca and/or Mg (likely from the breakdown of the carbonate target rock), though

further work needs to be conducted to say with confidence. To fully characterize the paragenetic sequence of this hydrothermal system and work towards constraining the timing and extent of hydrothermal activity at Flynn Creek crater, further microthermometry should be carried out on both fluorite and calcite, in addition to adularia and barite.

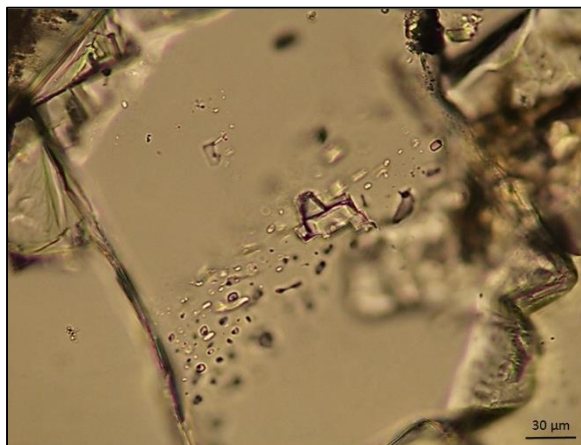


Figure 1. Photomicrograph of a fluid inclusion assemblage in fluorite (scale bar = 30 μm).

References: [1] Roddy, D.J. (1977a) In *Impact and Explosion Cratering* (eds. Roddy D.J. et al.), 125-161; [2] Roddy, D. J. (1977b) In *Impact and Explosion Cratering*, 277-308; [3] Evenick, J.C. (2006) Field Guide to the Flynn Creek Impact Structure. Knoxville: University of Tennessee. 22 pg; [4] Wilson, C.W., and Roddy, D.J. (1990, *TN Div. of Geo.*, 1:24,000 map; [5] Zahnle, K.J. and Sleep, N.H. (1997) In *Comets and the Origin and Evolution of Life*, edited by P. J. Thomas et al., pp. 175-208; [6] Kring, D.A. (2000) *GSA Today*, 10(8), 1-7; [7] Newsom, H.E. et al. (1996) *JGR*, 101, 14951-14956; [8] Schwenger, S.P. et al. (2012) *EPSL*, 335, 9-17; [9] Abramov, O. and Kring, D.A. (2005) *JGR*, 110, E12S09, doi:10.1029/2005JE002453. [10] Roddy, J.C. (1980) *LPSC 11*, #941. [11] Evenick, J.C., Lee, P., and Deane, B. (2004) *LPSC 35*, # 1131. [12] Osinski, G.R. et al. (2013) *Icarus* 224, 347-363.